


RESEARCH ARTICLE

Three in one: β -cyclodextrin, nanohydroxyapatite, and a nitrogen-rich polymer integrated into a new flame retardant for poly (lactic acid)

Henri Vahabi¹  | Meisam Shabaniyan² | Fezzeh Aryanasab² | Fouad Laoutid³ | Samira Benali³ | Mohammad Reza Saeb⁴  | Farzad Seidi⁵ | Baljinder K. Kandola⁶

¹Université de Lorraine, Laboratoire MOPS E. A. 4423, Metz F-57070, France

²Faculty of Chemistry and Petrochemical Engineering, Standard Research Institute (SRI), PO Box 31745-139, Karaj, Iran

³Center of Innovation and Research in Materials and Polymers (CIRMAP), Laboratory of Polymeric and Composite Materials (LPCM), University of Mons UMONS and Materia Nova Research Center, Place du Parc 20, 7000 Mons, Belgium

⁴Department of Resin and Additives, Institute for Color Science and Technology, PO Box: 16765-654, Tehran, Iran

⁵Department of Materials Science and Engineering, School of Molecular Science and Engineering, Vidyasirimedhi Institute of Science and Technology, 21210 Rayong, Thailand

⁶Institute for Materials Research and Innovation, University of Bolton, Bolton BL3 5AB, UK

Correspondence

Henri Vahabi, Université de Lorraine, Laboratoire MOPS E.A. 4423, Metz F-57070, France.

Email: henri.vahabi@univ-lorraine.fr

Meisam Shabaniyan, Faculty of Chemistry and Petrochemical Engineering, Standard Research Institute (SRI), Karaj, PO Box 31745-139, Iran. Email: m.shabaniyan@standard.ac.ir

Summary

A new halogen-free flame retardant was developed by integrating β -cyclodextrin, triazin ring, and nanohydroxyapatite (BSDH) into a hybrid system. A β -cyclodextrin was grafted to a commercially available SABO®STAB UV94 *via* an aromatic dehydratation. The BSDH was prepared in situ in the presence of β -cyclodextrin-grafted nitrogen-rich precursor. The resulting hybrid was applied as a flame retardant for poly(lactic acid) (PLA) and compared for performance with ammonium polyphosphate (APP). PLA composites containing BSDH and APP, individually or simultaneously, were examined for thermal degradation and flammability by TGA, cone calorimeter, and pyrolysis-combustion flow calorimetry. TGA results confirmed enhancement of thermal stability of PLA with assistance of BSDH compared to APP. The gases evolved during thermal degradation were assessed by a thermogravimetric analysis and Fourier infrared spectroscopy device. APP revealed catalytic effect to initiate PLA degradation, while BSDH continued to release some gases at elevated temperatures. The flame retardancy of PLA/APP/BSDH blend containing only 10 wt.% of additives was significantly improved. In cone calorimetric tests, a significant fall in peak of heat release rate was observed for this sample, 49% more than that of neat PLA, which was indicative of more gas and condensed phase reflected in more char residue. The corresponding PLA/APP sample, however, showed 17% improvement, as compared to neat PLA. Also, total heat release rate of PLA/APP/BSDH was 45 MJ.m⁻², whereas those of PLA and PLA/APP were 89 and 65 MJ.m⁻², respectively. BSDH and APP showed a synergistic effect on improving the flame retardancy of PLA composites.

KEYWORDS

flame retardancy, hydroxyapatite, poly (lactic acid), thermal degradation, β -cyclodextrin

1 | INTRODUCTION

Fire retardancy or conceivably fire prevention requirement has become a building block of choice of polymer materials. Poly (lactic acid) (PLA) lies among biopolymers widely used for packaging and biomedical applications thanks to its high stiffness, degree of transparency, and biocompatibility.¹⁻³ Recent progress in using PLA in electronics and construction has obliged engineers to improve flame retardancy of this versatile biopolymer.⁴ In this sense, a number of strategies as well as diverse flame retardant systems were practiced to develop PLA-based

systems guaranteeing a low fire risk.⁵⁻⁸ In spite of their high performance from a fire retardancy angle, halogenated fire retardants are being phased out nowadays because of the environmental issues associated with them. Consequently, the gas phase strategy predominant in halogenated flame retardants, which is based on quenching the flame in the gas phase *via* the formation of radical scavengers, is largely being replaced by condensed phase mechanisms to decline the amount of flammable products during combustion.⁹ Phosphorus-based flame retardant systems are efficient in polymer containing oxygen by formation of an insulating char layer, where phosphoric acid produced during

thermal decomposition condensate to produce pyrophosphate structures and form carbon-carbon double bonds *via* dehydration reaction of terminal alcohols at such an elevated temperature.^{10,11} Accordingly, a crosslinked or carbonized structure is formed to resist against burning.

To enhance their efficiency, phosphorus-based flame retardant additives are required to be assisted by char-forming agents,¹² nitrogen-based additives,¹³ or nanoparticles.¹⁴⁻¹⁶ Development of environmentally friendly PLA composites with the aid of green char-forming agents such as lignin, starch, cellulose, and β -cyclodextrin was the subject of different investigations.¹⁷⁻²³ It was also accepted that nanometric particles, depending on their chemical structure and geometry, can contribute to the enhancement of flame retardancy of polymers.⁷ Hydroxyapatite ($\text{Ca}_5(\text{OH})(\text{PO}_4)_3$, hereafter referred to as HA) has been applied in modification of flame retardancy of several polymers such as polyester, poly(methyl methacrylate), polycarbonate, and epoxy.²³⁻²⁵ HA belongs to bio-based crystalline calcium phosphate ceramics with a hexagonal structure composed of ca. 39 wt.% of Ca, 18.5 wt.% of P, and 3.38 wt.% of OH.^{26,27} It can be simply obtained through solvent extraction of bone bio-wastes.^{28,29} Surprisingly, enough HA was found in nanometric scale and contributed to improvement of both flame retardancy and mechanical properties of polymers.³⁰ Inspired by the literature,³¹ 3 flame retardants were encapsulated in a previous work as a flame retardant system and revealed synergistic performance towards EVA.³²

In the present work, a novel organic/inorganic additive was developed for PLA by integrating a nitrogen-rich polymer, a green cyclodextrin-based bowling agent, and a nanohydroxyapatite biomaterial into a hybrid flame retardant. The poly(β -cyclodextrin/SABO-ester-amide)/nano-hydroxyapatite compound was synthesized and characterized by thermogravimetric analysis (TGA) and Fourier infrared (FTIR) spectroscopy techniques. The individual and simultaneous effect of the developed hybrid in combination with ammonium polyphosphate (APP) on thermal and flammability behavior of the PLA was thoroughly discussed.

2 | MATERIALS AND METHODS

All chemicals used in this work were of analytical grade and available from commercial sources unless otherwise stated. A β -cyclodextrin, 3,3',4,4'-benzophenonetetracarboxylic dianhydride (BTDA), sodium hydride, calcium nitrate [$\text{Ca}(\text{NO}_3)_2 \cdot 4\text{H}_2\text{O}$], ammonium dihydrogen phosphate [$\text{NH}_4\text{H}_2\text{PO}_4$], and ammonia solution (25%) were all provided by Sigma Aldrich. SABO@STAB UV94 (SABO-Poly[[6-[(1,1,3,3-tetramethylbutyl)amino]-1,3,5-triazine-2,4-diy]][(2,2,6,6-tetramethyl-4-piperidinyl)imino]-1,6-hexanediy]][(2,2,6,6-tetramethyl-4-piperidinyl)imino]) was purchased from SABO S.p.A. Co. Poly(lactic acid) (PLA) was provided by Natureworks Co., Ingeo™ Biopolymer 3251D. Ammonium polyphosphate (APP), Exolit AP423, was purchased from Clariant.

2.1 | Synthesis of poly(β -cyclodextrin/SABO-ester-amide)/nanohydroxyapatite (BSDH)

Synthesis of poly(β -cyclodextrin/SABO-ester-amide)/nanohydroxyapatite (BSDH) was done through a 2-stage procedure. In the first stage, β -CD (2.270 g, 20.0 mmol) and dry DMF (30 ml) were added to a

500-mL round-bottomed flask fitted with a stirring bar. A solution of SABO (3.0 g) in dry DMF (20 mL) was then added to the mixture followed by dropwise NaOH (0.120 g, 5 mmol) addition in N_2 atmosphere. Stirring was continued at room temperature for a further 24 hours until a solution of BTDA (5.0 g, 15.5 mmol) in dry DMF (50 mL) was added dropwise, and the obtained solution was stirred for another 24 hours at 60°C. After the mixture remained from previous stage cooled down to room temperature, the resultant solid was filtered, washed carefully with DMF and acetone one after another followed by drying under vacuum for 12 hours. The resulting was poly(β -cyclodextrin/SABO-ester-amide), hereafter referred to as BSD. In the second stage, the BSDH was synthesized *in situ* using nanohydroxyapatite in the presence of BSD obtained in the previous stage. To do so, an aqueous solution of ammonium dihydrogen phosphate (2.750 g in 75-mL de-ionized water) was added to a well-dispersed mixture of the alkaline aqueous solution of $\text{Ca}(\text{NO}_3)_2$ (9.408 g in 75-mL de-ionized water). Then, BSD (6.0 g) was added under stirring prolonged for 24 hours at room temperature. The obtained solid was filtered and rinsed with water to keep the level of pH neutral, then dried at 80°C to attain BSDH. The previously mentioned procedure is schematically shown in Figure 1.

2.2 | PLA sample preparation

All composite samples were prepared in an internal mixer, Brabender-Haake, at 180°C, 60 rpm for 7 minutes. The samples were then grinded and hot-pressed using an Agila compression molding, under 6 MPa for 6 minutes at 200°C to obtain square sheets of $100 \times 100 \times 4 \text{ mm}^3$. The name and formulation of samples are given in Table 1.

2.3 | Characterization

Fourier transform infrared (FTIR) spectra were gathered on a Perkin-Elmer RXI spectrometer in the range of 400 to 4000 cm^{-1} with a resolution of 2 cm^{-1} . The X-ray diffraction (XRD) patterns were recorded using a Rigaku Miniflex II diffractometer with Cu K α radiation. The scanning range was 5° to 60° with a step size of 0.02° and step time of 1 second. All measurements were carried out using a 30-kV voltage and a 15-mA current. Transmission electron microscopy (TEM) micrographs were collected on a Philips CM100 apparatus using an acceleration voltage of 100 kV. Thermal gravimetric analysis (TGA) was carried out on a Setaram Labsys Evo thermogravimetric analyzer at a heating rate of 10°C.min⁻¹. The samples of approximately 20 mg were introduced in TGA Labsys Evo alumina crucible and analyzed under a nitrogen flow rate of 50 mL.min⁻¹ in a temperature interval ranging from ambient to 900°C. For gas analysis, TGA was coupled to a FTIR spectrometer (TGA-IR). Then, the identification of gases released directly during combustion analyzed from the degradation of samples using a Bruker Tensor 27 infrared spectrometer. The external TGA-IR module is equipped with a sensitive, liquid-nitrogen cooled mercuric cadmium telluride detector. Different parabolic and plane mirrors direct the IR light from the connected spectrometer through the gas cell to the mercuric cadmium telluride detector. Samples were scanned in the frequency range 800 to 4000 cm^{-1} at a resolution of 4 cm^{-1} and an accumulation of 32 scans. Fire behavior was investigated out using a

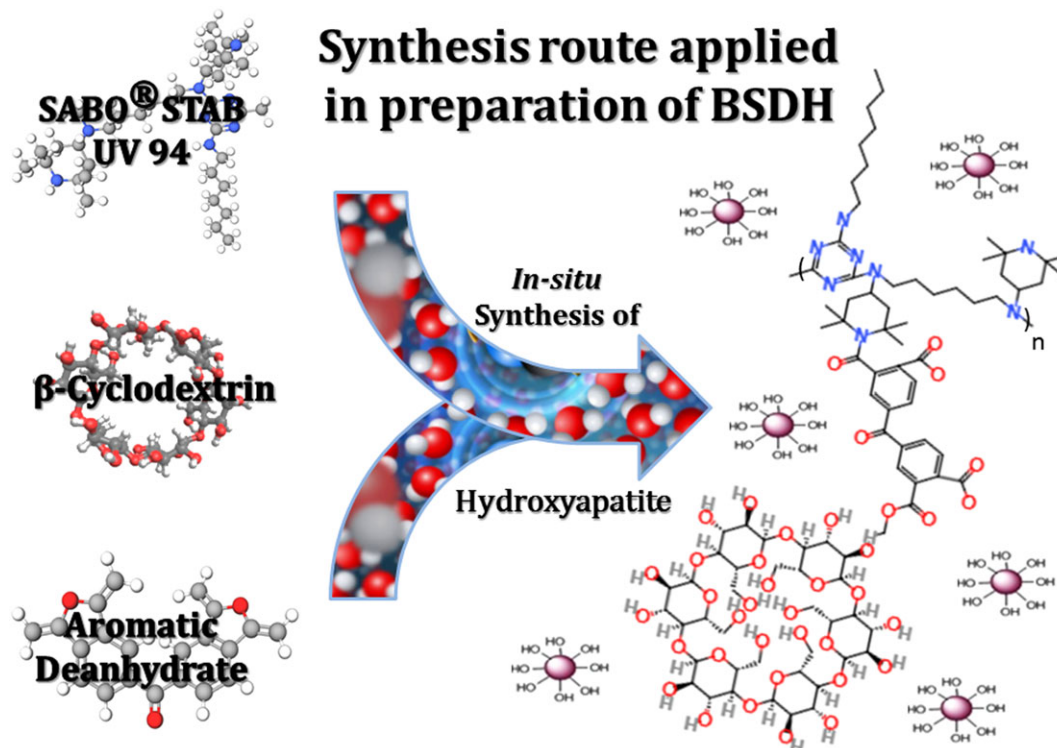


FIGURE 1 Synthesis procedure applied in this work for the preparation of BSDH [Colour figure can be viewed at [wileyonlinelibrary.com](#)]

TABLE 1 Name and composition of the samples prepared in this work

Sample code	PLA, wt.%	APP, wt.%	BSDH, wt.%
PLA	100	0	0
PLA/BSHDH	90	0	10
PLA/APP	90	10	0
PLA/APP/BSHDH	90	7.5	2.5

cone calorimeter by a Fire-EU-ISO5660 apparatus. The sheets ($100 \times 100 \times 4 \text{ mm}^3$ in size) were irradiated under 35 kW.m^{-2} . The parameters measured were heat release rate (HRR) and total heat release (THR). For each sample, the test was performed 3 times, where an experimental error of ca. 5% was considered as a reliable criterion. Pyrolysis combustion flow calorimeter (PCFC) was performed using an instrument from FTT Co. To do this test, specimens having weights between 2 and 4 mg were tested under heating rate of $^{\circ}\text{C.s}^{-1}$ in between 100°C and 750°C . Raman spectra were carried out using a Horiba Jobin Yvon Lab-RAM Aramis spectrophotometer fitted with a 532-nm laser and a 200-mm confocal pinhole. The laser was focused using a 10 objective. All spectra were obtained with an integration time of 30-second accumulation of 4 spectra recorded in the spectral range 800 to 2000 cm^{-1} .

3 | RESULTS AND DISCUSSION

3.1 | Characterization of BSDH

3.1.1 | Fourier transform infrared (FT-IR) analysis

The FTIR spectra of the β -CD, SABO, BSD, HA, and BSDH are compared in Figure 2. FTIR spectrum of BSD showed characteristic

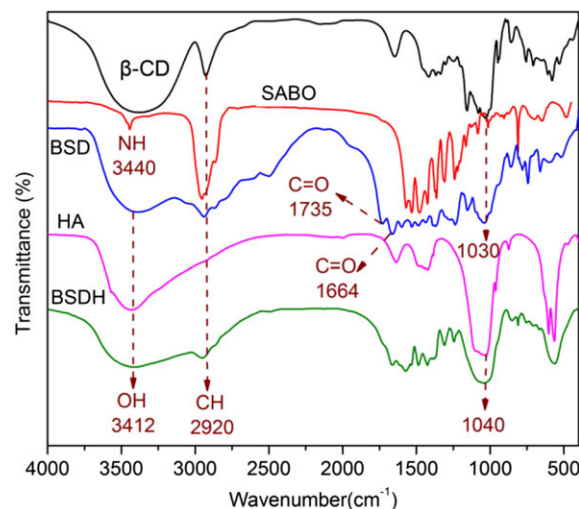


FIGURE 2 FTIR spectra of the synthesized β -CD, SABO, BSD, HA, and BSDH [Colour figure can be viewed at [wileyonlinelibrary.com](#)]

absorption bands of the β -CD and SABO structure conjointly with the absorption bands of the new carbonyl groups from formation of ester and amide groups (1735 and 1664 cm^{-1} , respectively) by BTDA crosslinker. In FTIR spectrum of HA, the absorption bands at 1043 , 604 , and 552 cm^{-1} correspond to the PO_4^{3-} . The strong OH bond (3436 cm^{-1}) is assigned to the stretching vibration of hydroxyl groups absorbed on the surface of HA. The FTIR spectrum of BSDH showed some absorption bands such as OH bond at 3410 cm^{-1} , the aliphatic C—H from β -CD and SABO at 2920 cm^{-1} , and the aromatic C=C and C=N from SABO and BTDA. The bands in the range 1150 to 1220 are attributed to C—O bonds of β -CD. In the FTIR spectrum of BSDH, the absorption bands at 1732 and 1664 cm^{-1} are assigned to C=O bonds of ester and amide or ketone groups.

3.1.2 | Assessment of BSDH structure and morphology

BSDH was analyzed by the XRD, whose diffraction pattern is shown in Figure 3A. The XRD patterns show maxima at $2\theta = 18.75^\circ$, 25.95° , 32.04° . The broad peak at 18.75° could be attributed to the amorphous region of BSD in the BSDH. The peaks at 25.95° and 32.04° correspond to HA.³³ Thus, the XRD patterns clearly confirm the presence of HA in the BSDH and successful synthesis of BSDH. In agreement with this, TEM image of BSDH reveals HA incorporated in BSDH in nanometric size, between 20 and 40 nm (Figure 3B).

3.1.3 | Thermal degradation of BSDH

TGA and DTG thermograms of the APP and BSDH under nitrogen atmosphere are displayed in Figure 4. The most important parameters extracted from thermal stability analysis (temperature at 5% mass loss: $T_{5\%}$, the temperature of the maximum weight loss: T_{\max} , as well as the amount of the final residue at 800°C) are summarized in Table 2. The thermal degradation of APP took place in 2 steps, where the corresponding T_{\max} of them peaked at 355°C and 682°C , respectively. The first step can be attributed to the release of NH_3 and H_2O leading to the formation of crosslinked polyphosphoric acids.^{34,35} The main degradation step that occurs during the second step corresponds to the formation of phosphorous oxides, P_4O_{10} and to the generation of a final residue of approximately 21% at 800°C . In the case of BSDH, 3 decomposition steps were detected (T_{\max} of 135, 305, and 445°C). The first degradation can be ascribed to a weight loss of approximately

TABLE 2 TGA parameters of samples in nitrogen (*maximum weight loss temperature, obtained from DTG)

Sample code	$T_{5\%}$, $^\circ\text{C}$	T_{\max} , $^\circ\text{C}$	Residue at 800°C (wt.%)
PLA	335	368	0
APP	354	355 682	21
BSDH	164	135 305 445	59
PLA/BSHDH	334	364	12
PLA/APP	326	360	15
PLA/APP/BSHDH	323	361	11

8%, which is probably a signature of release of the absorbed water or water of crystallization (complexed water inside the cavity) expecting from β -cyclodextrin dehydration.^{36,37} The second weight loss occurs between 220°C and 390°C which is equivalent of 15% of weight loss. The third degradation step takes place between 390°C and 700°C corresponding to 20% weight loss. It is apparent that BSDH is less thermally stable with respect to APP, but its thermal degradation enables for obtaining higher amount of char residue (59% in comparison with 21% generated by APP).

3.2 | Characterization of PLA composites

Thanks to its high residue remained from TGA test; BSDH could present some advantages for improving char formation during the combustion of PLA. With this in view, 10 wt% of BSDH was incorporated into

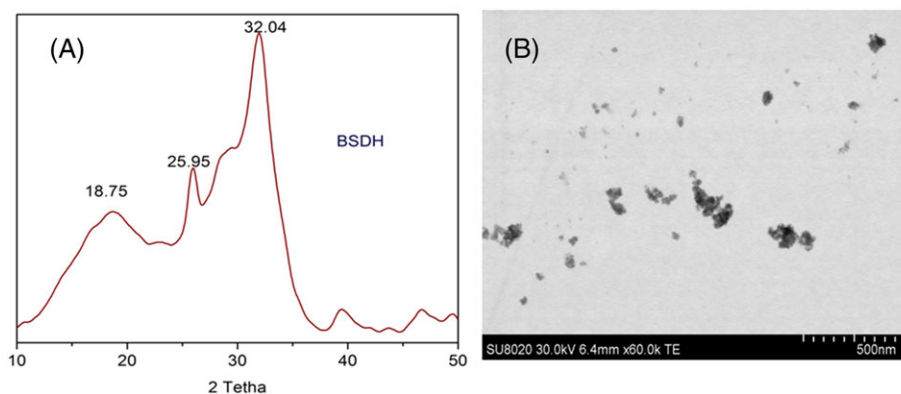


FIGURE 3 XRD diffraction pattern (A) and TEM image (B) of the synthesized BSDH [Colour figure can be viewed at wileyonlinelibrary.com]

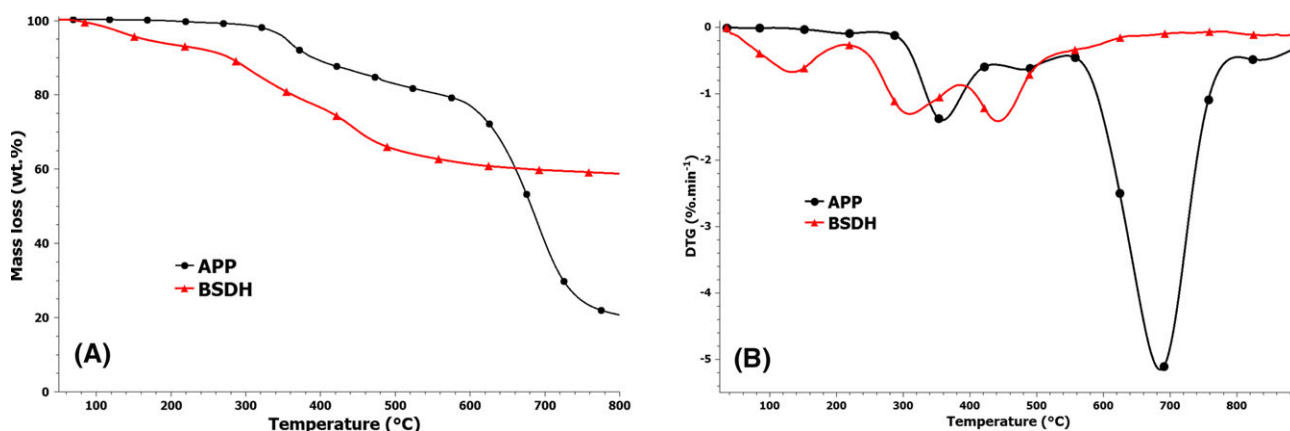


FIGURE 4 TGA (A) and DTG (B) curves of APP and BSDH in nitrogen [Colour figure can be viewed at wileyonlinelibrary.com]

PLA and its dispersion state in the matrix as well as its effects on both thermal and fire behavior of PLA were investigated. The performances of systems were with those obtained with PLA containing 10 wt.% APP and an equivalent amount of a blend of APP (7.5 wt.%) and BSDH (2.5 wt.%).

3.2.1 | Morphology observations of composites

The dispersion state of the fire-retardant additives throughout the PLA matrix is an important parameter affecting the flame retardant behavior of composite. Figure 5 shows TEM images of PLA/BSDH sample. It can be seen that HA nanoparticles are homogeneously dispersed within PLA in the absence of aggregates, verifying good compatibility of BSDH with PLA.

3.2.2 | Thermogravimetric analysis (TGA)

TGA thermograms of PLA and PLA-based composites are shown in Figure 6. The detailed TGA data are summarized in Table 2. Overall, it can be recognized from the curves that all samples decomposed through a 1-step-degradation. Compared with the thermal decomposition behavior of the neat PLA, the PLA/APP and PLA/APP/BSDH specimens showed lower thermal stability. The onset temperature ($T_{5\%}$) of

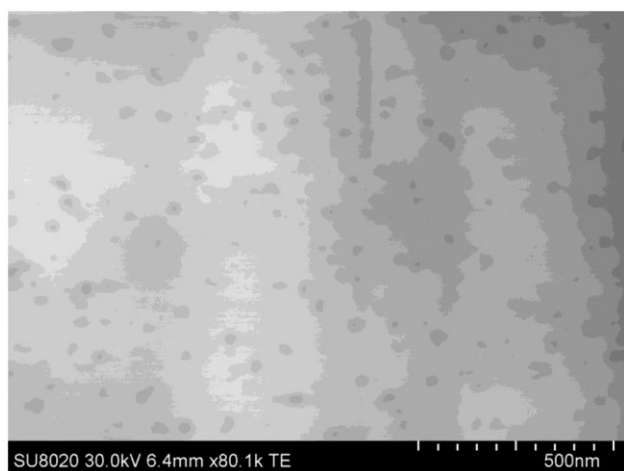


FIGURE 5 TEM image of the PLA/BSDH composite

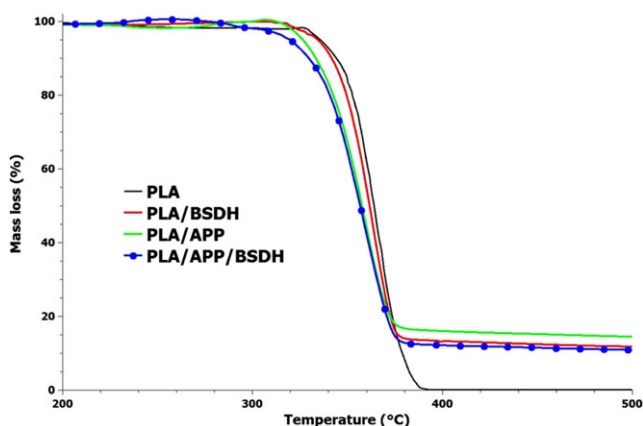


FIGURE 6 TGA curves of samples obtained at heating rate of $10^{\circ}\text{C}\cdot\text{min}^{-1}$ under nitrogen atmosphere [Colour figure can be viewed at wileyonlinelibrary.com]

PLA/BSDH sample was almost similar to that of the neat PLA. Because BSDH presented lower thermal stability than that of PLA or APP (Table 2), its incorporation into the PLA was supposed to negatively affect the thermal stability of composite. Surprisingly, however, it was observed that BSDH had a positive effect on thermal stability of PLA. It means that there are complex interactions between the BSDH and PLA. The formation of a residue was observed for all samples above 375°C , except for the neat PLA that burnt completely. The final residue rates were 12%, 15%, and 11% for PLA/BSDH, PLA/APP, and PLA/APP/BSDH samples, respectively. Moreover, there was no improvement in the char residue after blending BSDH and APP ingredients.

The FTIR spectra of the evolved gases were continuously recorded during TGA experiments at heating rate of $10^{\circ}\text{C}\cdot\text{min}^{-1}$ for the PLA/BSDH, PLA/APP, and PLA/APP/BSDH samples. The FTIR data were obtained around DTG peaks, the temperature at which degradation was initiated (at 315°C , T_{max} and end degradation temperature (385°C) (Figure 7). From the FTIR spectra at 315°C , it is clear that the PLA systems containing APP were degraded even in the presence of BSDH. This is while PLA/BSDH sample did not show any absorption band at the assigned temperature. It is observed that PLA/APP and PLA/APP/BSDH have almost the same bands with the same intensities. In Figure 7A, the absorption band at 1118 cm^{-1} is attributed to the C–O stretching vibration, while the ones at 1416 and 1371 cm^{-1} are attributed to the C–H bending vibration of CH_3 . The absorption bands recorded at 1760 cm^{-1} are assigned to the C=O stretching vibration, and the bands at 2109 and 2185 cm^{-1} can be attributed to C≡O group. The band at 2311 and 2362 cm^{-1} corresponds to CO_2 . The broad band appeared in between 2600 and 3100 cm^{-1} corresponds to OH of COOH groups. Overall, the absorption bands demonstrated that during PLA degradation acetaldehyde, acetic acid, CO_2 , CO, and H_2O should be released.^{38–40} Release of the gases such as acetaldehyde, acetic acid, and CO_2 is due to degradation of PLA and gives rise to the conclusion that APP has catalytic effect on degradation of PLA. Unlike the FTIR spectrum at 315°C , PLA/BSDH showed the highest degradation at T_{max} (Figure 7B). PLA/APP and PLA/APP/BSDH showed almost the same adsorption bands except in the range of 1315 to 1560 cm^{-1} , which could be corresponded to the presence of BSDH. There is a sharp absorption band at 1789 cm^{-1} in the FTIR spectrum of PLA/BSDH specimen corresponding to C=O groups. The bands of CO and CO_2 are also observed in the range between 2050 and 2408 cm^{-1} . The absorption bands at 2893 and 2964 cm^{-1} are attributed to C–H stretching vibration of aliphatic CH_2 or CH_3 groups. The absorption band at 3005 cm^{-1} is corresponded to C–H of aldehyde group. It can be concluded from FTIR spectrum of PLA/BSDH that formaldehyde and acetaldehyde along with CO_2 and CO are the main gases released. FTIR spectra of samples at 385°C are shown in Figure 6C. From FTIR spectrum of PLA/APP, it is apparent that at the corresponding temperature, the degradation rate obviously decreased, whereas FTIR spectra of the PLA/APP/BSDH and PLA/BSDH underwent a similar pathway, as compared with FTIR spectra of these samples at the T_{max} . This suggests that BSDH remained thermally stable until reaching a state to release the gases at 385°C . From this angle, APP helps to release the gases at lower temperatures, while BSDH continues the release of gases at higher temperature.

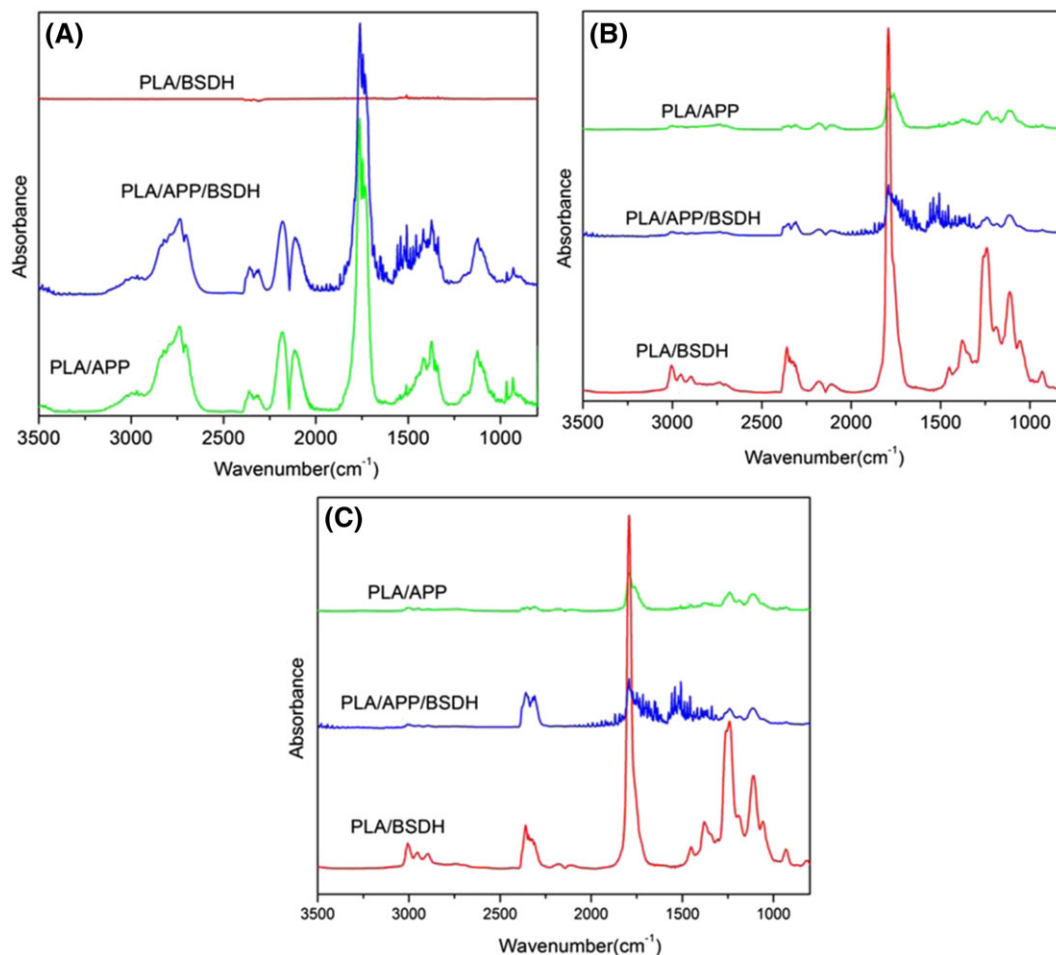


FIGURE 7 FTIR spectra of the evolved gases during TGA, for PLA/BSHD, PLA/APP, and PLA/APP/BSHD samples at 315°C (A), T_{max} (B), and 380°C (C) [Colour figure can be viewed at wileyonlinelibrary.com]

3.2.3 | Cone calorimeter

Figure 8 shows and compares the HRR curves obtained from cone calorimeter tests. The statistics of pHRR and THR relating to the cone calorimeter tests are also given in Table 3. The pHRR values of PLA and PLA/BSHD show a similar tendency (365 kW.m⁻²). However, PLA/APP showed a limited reduction in the pHRR value down to 302 kW.m⁻². On the other hand, at the end of burning, neat PLA has released a total heat of 89 MJ.m⁻², while the THR values of PLA/BSHD and

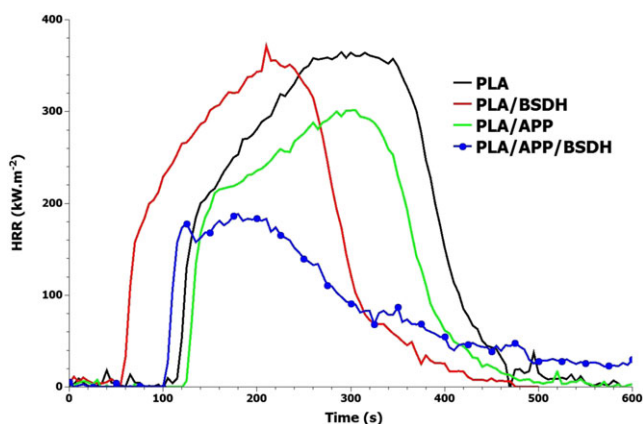


FIGURE 8 HRR curves obtained from cone calorimeter tests under an incident heat flux of 35 kW.m⁻² [Colour figure can be viewed at wileyonlinelibrary.com]

TABLE 3 Summary of the statistics of the cone calorimeter tests

	pHRR, kW.m ⁻²	THR, MJ.m ⁻²	TTI, s	Residue, wt.%	Reduction in pHRR, %
PLA	365	89	110	0	-
PLA/BSHD	365	73	55	5	0
PLA/APP	302	65	124	15	17
PLA/APP/BSHD	185	45	101	40	49

PLA/APP were 73 and 65 MJ.m⁻², respectively. In order to further improve the flame retardancy of the composites, BSDH and APP were simultaneously introduced into the PLA with a total loading of 10 wt%. With this combination, the flame retardancy of PLA/APP/BSHD showed an acceptable synergist effect compared to the neat PLA, as signaled by a considerable fall in pHRR and THR quantities. From Table 3, it can be seen that PLA/APP/BSHD shows a relatively low pHRR value compared to the other 2 systems. The simultaneous use of APP and BSDH appeared efficient for flame retardancy improvement. Regarding the decrease of pHRR, a reduction of ca. 49% was observed for PLA/APP/BSHD sample compared to the neat PLA. In a similar fashion, the THR value of PLA/APP/BSHD showed a significant reduction in comparison with the neat PLA. The shape of HRR curve was evidently changed for this sample. It should be noticed that the total time of combustion was extended when APP or BSDH was added. Compared to the TTI value of PLA (110 s), PLA/APP and PLA/

BSDH showed TTI values of 124 and 55 seconds, respectively. The reduction in TTI of PLA/ BSDH could be due to the presence of thermally sensitive groups such as cyclodextrin and aliphatic amine in the structure of BSDH, the results are consistent with TGA results where it was seen that BSDH starts losing mass at lower temperatures than APP. The TTI for PLA/APP/ BSDH was shortened to 101 seconds. The results suggest that combination of APP and BSDH could give rise to an acceptable TTI with respect to that of the neat PLA.

Mass loss curves obtained from cone calorimeter tests are presented in Figure 9. The residue content was around 5% and 15% for PLA/ BSDH and PLA/APP samples, respectively. However, in PLA/APP/ BSDH. The residue content increased to approximately 37%. Moreover, the formed char residue seems to be thermally stable after 200°C compared to the other samples. Therefore, it can be assumed that the reduction of the amount of volatile compounds, owing to the formation of such thermally stable residue, is the key parameter explaining the important decrease of the pHRR obtained when APP and BSDH are combined. Taking into account these results, it appears thus that neither BSDH nor APP is capable of imparting relevant flame retardant behavior to PLA. However, the combination of both additives significantly reduced PLA's flammability, probably due to the nanometric form of BSDH. The combination of nanoparticles with conventional flame retardant additives, and especially with phosphorous based ones, has been reported, in some cases, to allow reaching better performances.⁴¹

The superposition of HRR (obtained from PCFC tests) and DTG (obtained from TGA tests) curves for all the samples is displayed in Figure 10. This type of curve superposition lets us investigate about the energetic value of released gases in PCFC compared to the quantity of released gases in TGA.⁴²⁻⁴⁴ Both analyses (PCFC and TGA) were made under nitrogen atmosphere. The observed shift between HRR and DTG curves is related to the different constants of heating rate in TGA ($10^{\circ}\text{C}\cdot\text{min}^{-1}$) and PCFC ($1\text{ K}\cdot\text{s}^{-1}$) analysis. The shape of PCFC (black dashed line) and DTG (black line) curves as well as their height is similar for pure PLA. Therefore, it can be concluded that the energetic value of released gases is proportional to the quantity of the released gases for pure PLA. On the other hand, there is a gap between these values for other samples, as shown in Figure 10 with double

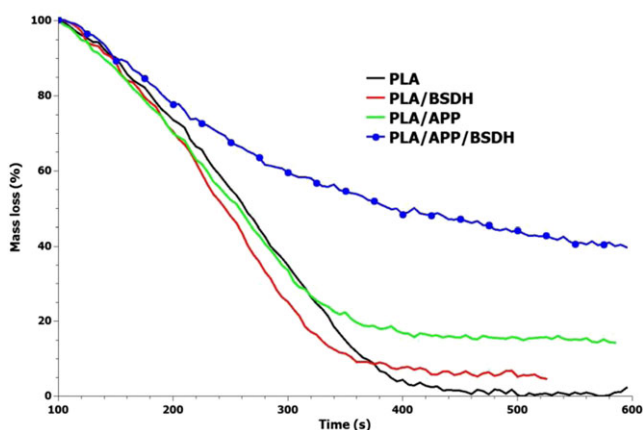


FIGURE 9 Mass loss curves as a function of time for all samples, obtained from cone calorimeter tests [Colour figure can be viewed at [wileyonlinelibrary.com](#)]

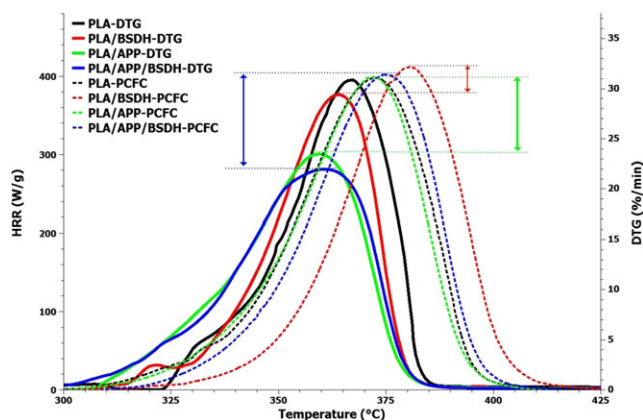


FIGURE 10 Superposition of HRR (dashed lines), obtained from PCFC tests, and DTG (solid lines) curves as a function of temperature for all samples [Colour figure can be viewed at [wileyonlinelibrary.com](#)]

headed arrows. The difference could be explained by the different amount of char formed because the variation of pHRR in PCFC for different samples is not important. Therefore, it can be concluded that the vapor phase action is less than that of condensed phase. Thus, in the case of cone calorimeter test when condensed phase plays an important role, the flame retardancy of PLA/APP/ BSDH sample owing to increased char formation was improved.

3.2.4 | Characterization of the residual char

Combining BSDH and APP enables for the formation of a high amount of thermally stable char. This protective carbonaceous char may act as a thermal barrier to prevent polymer degradation and also avoids the transfer of flammable gases to vapor phase and penetration of oxygen into condensed phases during combustion.⁴⁵ Insulation character of char residue can be evaluated from its properties such as cohesion, morphology, thickness, and porosity.^{46,47} Therefore, the remaining carbonaceous residues after cone calorimeter tests were investigated using XRD and Raman spectroscopy.

3.2.5 | Structure of residue

Figure 11 shows the macroscopic digital photographs of the char residue formation at the end of cone calorimeter tests. PLA completely burns without any residue. The remaining residue of PLA/ BSDH is quite limited and is of a powder-like form that cannot act as an effective char layer (Figure 11A). PLA/APP showed a char layer but with some holes and is of low quality. The char structure seems more cohesive for the sample containing both APP and BSDH (Figure 11C). An intumescent behavior was also observed for PLA/APP/ BSDH sample. As compared with that of PLA/APP, the quality of char layered is obviously improved in PLA/APP/ BSDH. The char is thicker for this sample, and a more important char swelling was obtained compared to the other samples. This excellent intumescent char residue layer could limit the combustible released gases, act as a thermal insulation and heat feedback from the fire, and also away oxygen from burning materials. Thus, this thick char produces a more efficient fire protective barrier and therefore a better flame retardancy for this sample.

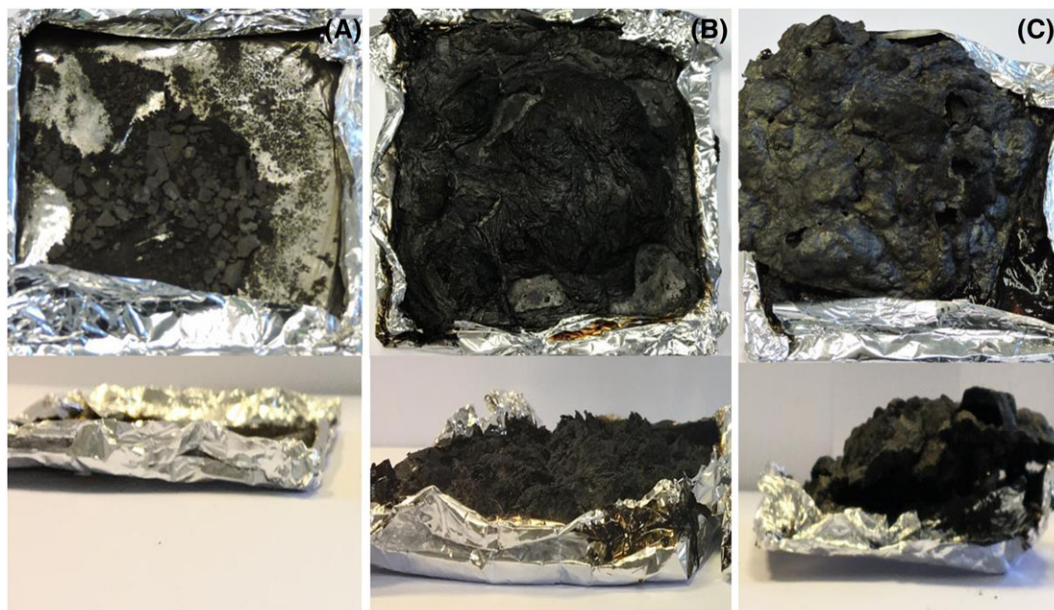


FIGURE 11 Photographs of the residues remaining after the cone calorimeter test in 2 sides, (A) PLA/BSHD, (B) PLA/APP, and (C) PLA/APP/BSHD [Colour figure can be viewed at wileyonlinelibrary.com]

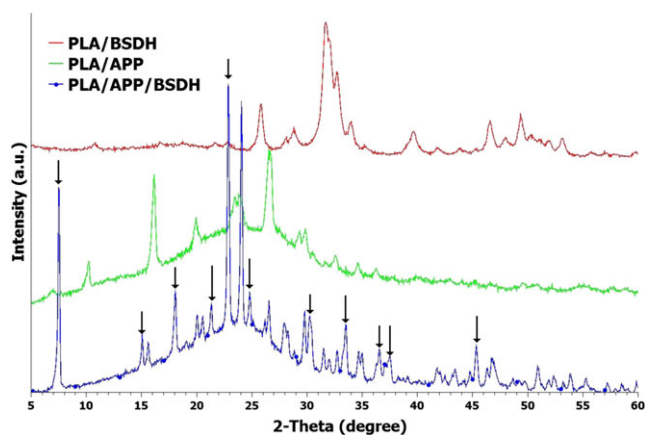


FIGURE 12 XRD patterns of remaining residues after the cone calorimeter for PLA/BSHD, PLA/APP, and PLA/APP/BSHD samples [Colour figure can be viewed at wileyonlinelibrary.com]

3.2.6 | X-ray diffraction analysis of the residues

The formation of new crystalline phase structures during combustion contributes to reinforcement and therefore efficiency of insulating char on the surface of polymer.⁴⁸ As described earlier, this insulating barrier leads to better flame retardancy. The XRD patterns of residues after cone calorimeter tests for PLA/BSHD, PLA/APP, and PLA/APP/BSHD samples are shown in Figure 12. It can be seen that some new peaks have appeared in PLA/APP/BSHD, as compared to the PLA/APP and PLA/BSHD samples. This is a clear evidence of the formation of some new crystalline structures as a result of an interaction between the 2 compounds during the combustion. This could improve the char quality.

A possible interaction between APP and BSDH during the combustion can be illustrated in Figure 13. The interaction can take place between APP and β -cyclodextrine part of molecule as well as SABO side of BSDH. These interactions can modify the char quality and therefore flame retardancy.

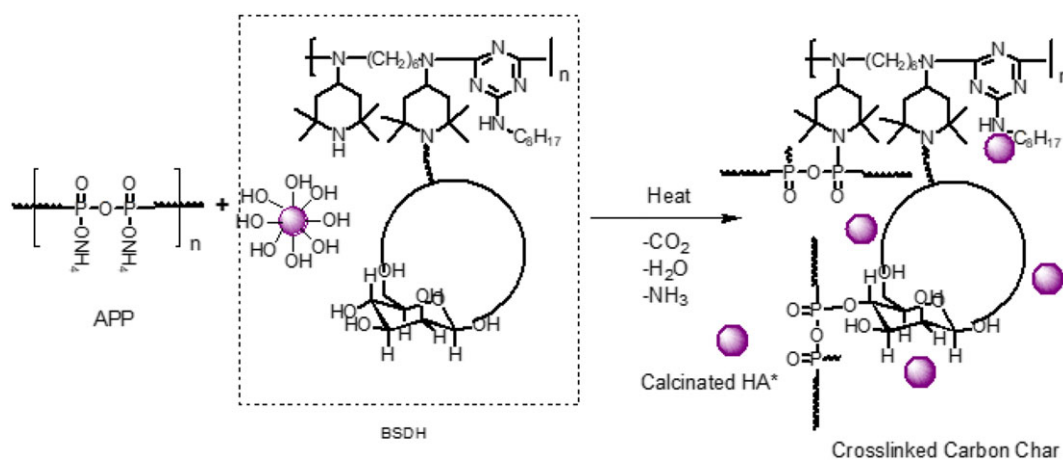


FIGURE 13 Schematic showing the possible interactions between APP and BSDH during the combustion (*HA: Hydroxyapatite) [Colour figure can be viewed at wileyonlinelibrary.com]

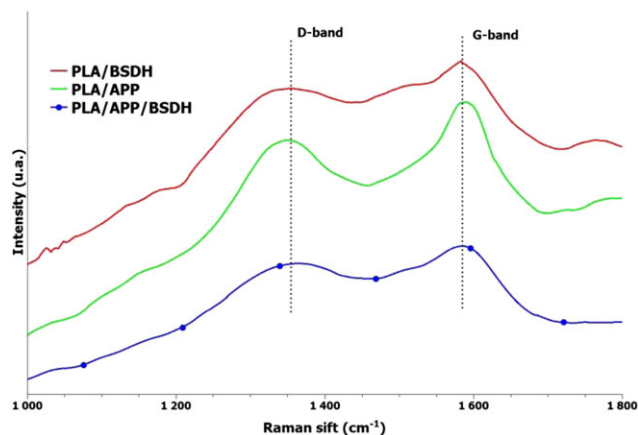


FIGURE 14 Raman spectra of residues after the cone calorimeter for PLA/BSDH, PLA/APP, and PLA/APP/BSDH samples [Colour figure can be viewed at wileyonlinelibrary.com]

3.2.7 | Raman spectroscopy of the residues

The characterization of structural order degree of carbonaceous char was performed using Raman spectroscopy. The increase of graphitization degree of the residual char can provide efficient thermal insulation, which results in an effective decrease in the degradation of polymer and heat transfer between the flame and the materials. Raman spectra of residues after the cone calorimeter test for PLA/BSDH, PLA/APP, and PLA/APP/BSDH samples are presented in Figure 14. Two absorption bands at 1350 and 1590 cm^{-1} , which are named D and G bands, respectively, are present in the spectra of these samples. According to the literature, the graphitization degree of char can be estimated by calculating the ratio between the integrated intensities of D and G bands.^{49,50} The decrease of this ratio (I_D/I_G) is expected with increase of graphitization. The I_D/I_G value is 1.72, 1.56, and, 1.48 for PLA/BSDH, PLA/APP, and PLA/APP/BSDH, respectively. It can be concluded that obtained char of PLA/APP/BSDH has the highest graphitization degree. Besides the fact that combining BSDH and APP leads to the formation of higher char amount (Figure 11 and Table 3), this combination enables also improving its quality as evidenced by Raman spectroscopy.

4 | CONCLUSIONS

In this work, a novel organic-inorganic hybrid containing amine, triazine, cyclodextrin, and nano-hydroxypaptite was synthesized for the first time via grafting of β -cyclodextrin to the SABO®STAB UV94 via an aromatic dehydrate along with in-situ preparation of nanohydroxyapatite on its surface. The new flame retardant was melt blended alone and in combination with APP into PLA matrix in order to improve latter's flame retardancy. The TGA results showed that thermal stability of the PLA and PLA/BSDH samples was almost same while the samples containing APP including PLA/APP and PLA/APP/BSDH showed an obvious decreasing in thermal stability as compared to the neat PLA. It was also observed that char residue is not the only way to improve flame retardancy of PLA/APP/BSDH. From TGA coupled FTIR results, it was observed that APP has a catalytic effect on degradation of PLA and releases some gases and BSDH continued release the gases at

high temperatures. Thus, a continuous gas phase action may bring a better flame retardancy. The flame retardant properties of the PLA composites investigated by cone calorimetry indicated that by introducing 2.5 wt.% BSDH into the PLA/APP system, an excellent synergistic effect for improving the flame retardancy was observed in PLA/APP/BSDH sample, demonstrated by a significant reduction in pHRR and THR values. The investigation of condensed and vapor phases, using XRD, Raman, PCFC, and TGA/FTIR, showed that the principal action is essentially in condensed phase. PLA/APP/BSDH sample showed a higher temperature range of gas release and high char residue with good quality as compared to the other samples.

ACKNOWLEDGEMENTS

The authors wish to thank the technological platform "Plastinnov" at the University of Lorraine for their support in the preparation of samples and fire tests.

ORCID

Henri Vahabi  <http://orcid.org/0000-0003-0419-7368>

Mohammad Reza Saeb  <http://orcid.org/0000-0001-7860-5243>

REFERENCES

- Södergård A, Stolt M. Properties of lactic acid based polymers and their correlation with composition. *Prog Polym Sci.* 2002;27(6):1123-1163.
- Auras R, Harte B, Selke S. An overview of polylactides as packaging materials. *Macromol Biosci.* 2004;4(9):835-864.
- Inkinen S, Hakkarainen M, Albertsson A-C, Södergård A. From lactic acid to poly (lactic acid)(PLA): characterization and analysis of PLA and its precursors. *Biomacromolecules.* 2011;12(3):523-532.
- V.K.K.V.Y. Horikoshi. Bio-based polymers. *Fujitsu Sci Tech J.* 2005;41:173-180.
- Bourbigot S, Fontaine G. Flame retardancy of polylactide: an overview. *Polym Chem.* 2010;1(9):1413-1422.
- Wang X, Wang D. Fire-retardant polylactic acid-based materials: preparation, properties, and mechanism. In: *Novel Fire Retardant Polymers and Composite Materials.* Vol.93. Woodhead publishing, Elsevier, Ltd.; 2016.
- Shabanian M, Kang N-J, Wang D-Y, Wagenknecht U, Heinrich G. Synthesis of aromatic-aliphatic polyamide acting as adjuvant in polylactic acid (PLA)/ammonium polyphosphate (APP) system. *Polym Degrad Stab.* 2013;98(5):1036-1042.
- Shabanian M, Hajibeygi M, Hedayati K, Khaleghi M, Khonakdar HA. New ternary PLA/organoclay-hydrogel nanocomposites: design, preparation and study on thermal, combustion and mechanical properties. *Mater Des.* 2016;110:811-820.
- Mitchell JW. The history and future trends of non-halogenated flame retarded polymers. In: Morgan AB, Wilkie CA, eds. *Non-Halogenated Flame Retardant Handbook.* Scrivener Publishing, Wiley; 2014:1-16.
- Weil E. *Encyclopedia of Polymer Science and Technology.* New York: Wiley Interscience; 1986.
- Aaronson AM. *Phosphorus Flame Retardants for a Changing World.* ACS Publications; 1992.
- Sawada Y, Yamaguchi J, Sakurai O, Uematsu K, Mizutani N, Kato M. Thermogravimetric study on the decomposition of hydromagnesite 4 $\text{MgCO}_3 \cdot \text{Mg}(\text{OH})_2 \cdot 4 \text{H}_2\text{O}$. *Thermochimica acta.* 1979;33:127-140.
- Rigolo M, Woodhams R. Basic magnesium carbonate flame retardants for polypropylene. *Polym Eng Sci.* 1992;32:327-334.
- Haurie L, Fernández AI, Velasco JI, Chimenos JM, Cuesta J-ML, Espiell F. Synthetic hydromagnesite as flame retardant. Evaluation of the flame

- behaviour in a polyethylene matrix. *Polym Degrad Stab.* 2006;91(5):989-994.
15. Haurie L, Fernández AI, Velasco JI, Chimenos JM, Ticó-Grau JR, Espiell F. Synthetic hydromagnesite as flame retardant. A study of the stearic coating process. *Macromolecular Symposia*, Wiley Online. *Library.* 2005;165-174.
 16. Levchik SV. Introduction to flame retardancy and polymer flammability. In: Morgan AB, Wilkie CA, eds. *Flame Retardant Polymer Nanocomposites*. Hoboken, NJ, USA: John Wiley & Sons, Inc; 2007:1-29.
 17. Reti C, Casetta M, Duquesne S, Bourbigot S, Delobel R. Flammability properties of intumescent PLA including starch and lignin. *Polym Adv Technol.* 2008;19(6):628-635.
 18. Costes L, Laoutid F, Aguedo M, et al. Phosphorus and nitrogen derivatization as efficient route for improvement of lignin flame retardant action in PLA. *Eur Polym J.* 2016;84:652-667.
 19. Zhan J, Song L, Nie S, Hu Y. Combustion properties and thermal degradation behavior of polylactide with an effective intumescent flame retardant. *Polym Degrad Stab.* 2009;94(3):291-296.
 20. Feng JX, Su SP, Zhu J. An intumescent flame retardant system using β -cyclodextrin as a carbon source in polylactic acid (PLA). *Polym Adv Technol.* 2011;22(7):1115-1122.
 21. Zhang R, Xiao X, Tai Q, Huang H, Hu Y. Modification of lignin and its application as char agent in intumescent flame-retardant poly (lactic acid). *Polym Eng Sci.* 2012;52(12):2620-2626.
 22. Wang B, Qian X, Shi Y, et al. Cyclodextrin microencapsulated ammonium polyphosphate: preparation and its performance on the thermal, flame retardancy and mechanical properties of ethylene vinyl acetate copolymer. *Compos Part B Eng.* 2015;69:22-30.
 23. Elbasaney S, Mostafa HE. Synthesis and surface modification of nanophosphorous-based flame retardant agent by continuous flow hydrothermal synthesis. *Particuology.* 2015;22:82-88.
 24. Dong QX, Chen QJ, Yang W, et al. Thermal properties and flame retardancy of polycarbonate/hydroxyapatite nanocomposite. *J Appl Polym Sci.* 2008;109(1):659-663.
 25. Dholakiya BZ. Use of non-traditional fillers to reduce flammability of polyester resin composites. *polimeri.* 2009;30:10-17.
 26. Higashi S, Yamamuro T, Nakamura T, Ikada Y, Hyon S-H, Jamshidi K. Polymer-hydroxyapatite composites for biodegradable bone fillers. *Biomaterials.* 1986;7(3):183-187.
 27. Blazewicz S. Bioactive polymer/hydroxyapatite (nano) composites for bone tissue regeneration. In: *Biopolymers*. Berlin Heidelberg: Springer-Verlag; 2010:97-207.
 28. Barakat NA, Khil MS, Omran A, Sheikh FA, Kim HY. Extraction of pure natural hydroxyapatite from the bovine bones bio waste by three different methods. *J Mater Process Technol.* 2009;209(7):3408-3415.
 29. Brzezińska-Miecznik J, Haberk K, Sitarz M, Bućko MM, Macherzyńska B. Hydroxyapatite from animal bones—extraction and properties. *Ceram Int.* 2015;41 (4841-4846).
 30. Zebarjad SM, Sajjadi SA, Sdrabadi TE, Sajjadi S, Yaghmaei A, Naderi B. A study on mechanical properties of PMMA/hydroxyapatite nanocomposite. *Engineering.* 2011;3(08):795-801.
 31. Laoutid F, Bonnaud L, Alexandre M, Lopez-Cuesta J-M, Dubois P. New prospects in flame retardant polymer materials: from fundamentals to nanocomposites. *Mater Sci Eng R Rep.* 2009;63(3):100-125.
 32. Vahabi H, Raveshatian A, Fasihi M, et al. Competitiveness and synergy between three flame retardants in poly (ethylene-co-vinyl acetate). *Polym Degrad Stab.* 2017;143:164-175.
 33. Annaz B, Hing K, Kayser M, Buckland T, Di Silvio L. An ultrastructural study of cellular response to variation in porosity in phase-pure hydroxyapatite. *J Microsc.* 2004;216(2):97-109.
 34. Camino G, Costa L, Trossarelli L. Study of the mechanism of intumescence in fire retardant polymers: part I—thermal degradation of ammonium polyphosphate-pentaerythritol mixtures. *Polym Degrad Stab.* 1984;6(4):243-252.
 35. Ni J, Chen L, Zhao K, Hu Y, Song L. Preparation of gel-silica/ammonium polyphosphate core-shell flame retardant and properties of polyurethane composites. *Polym Adv Technol.* 2011;22(12):1824-1831.
 36. Trotta F, Zanetti M, Camino G. Thermal degradation of cyclodextrins. *Polym Degrad Stab.* 2000;69(3):373-379.
 37. Song LX, Teng CF, Xu P, Wang HM, Zhang ZQ, Liu QQ. Thermal decomposition behaviors of β -cyclodextrin, its inclusion complexes of alkyl amines, and complexed β -cyclodextrin at different heating rates. *J Incl Phenom Macrocycl Chem.* 2008;60(3-4):223-233.
 38. Tudorachi N, Lipsa R, Mustata FR. Thermal degradation of carboxymethyl starch-g-poly (lactic acid) copolymer by TG-FTIR-MS analysis. *Ind Eng Chem Res.* 2012;51(48):15537-15545.
 39. Zou H, Yi C, Wang L, Liu H, Xu W. Thermal degradation of poly (lactic acid) measured by thermogravimetry coupled to Fourier transform infrared spectroscopy. *J Therm Anal Calorim.* 2009;97(3):929-935.
 40. Dhar P, Katiyar V. Thermal degradation kinetics of polylactic acid/acid fabricated cellulose nanocrystal based bionanocomposites. *Int J Biol Macromol.* 2017;104:827-836.
 41. Intrater J. In: Morgan A, Wilkie C, eds. *A Review of Flame Retardant Polymer Nanocomposites*. Hoboken, New Jersey: John Wiley & Sons, Inc.; 2007:421. ISBN:978-0-471-73426-0, Taylor & Francis 2008.
 42. Vahabi H, Longuet C, Ferry L, David G, Robin JJ, Lopez-Cuesta JM. Effect of aminobisphosphonated copolymer on the thermal stability and flammability of poly (methyl methacrylate). *Polym Int.* 2012;61(1):129-134.
 43. Schartel B, Pawlowski KH, Lyon RE. Pyrolysis combustion flow calorimeter: a tool to assess flame retarded PC/ABS materials? *Thermochimica Acta.* 2007;462(1-2):1-14.
 44. Morgan AB, Galaska M. Microcombustion calorimetry as a tool for screening flame retardancy in epoxy. *Polym Adv Technol.* 2008;19(6):530-546.
 45. Morgan AB, Cusack PA, Wilkie CA. Other non-halogenated flame retardant chemistries and future flame retardant solutions. In: Morgan AB, Wilkie CA, eds. *Non-Halogenated Flame Retardant Handbook*. Scrivener Publishing, Wiley; 2014:347-403.
 46. Muller M, Bourbigot S, Duquesne S, et al. Investigation of the synergy in intumescent polyurethane by 3D computed tomography. *Polym Degrad Stab.* 2013;98(9):1638-1647.
 47. Jaramillo M, Koo J, Natali M. Compressive char strength of thermoplastic polyurethane elastomer nanocomposites. *Polym Adv Technol.* 2014;25(7):742-751.
 48. Friederich B, Laachachi A, Ferriol M, Ruch D, Cochez M, Toniazzo V. Improvement of thermal stability and fire behaviour of PMMA by a (metal oxide nanoparticles/ammonium polyphosphate/melamine polyphosphate) ternary system. In: *Integrated Systems, Design and Technology 2010*. Berlin, Heidelberg: Springer; 2011:47-58.
 49. Feng C, Liang M, Jiang J, Huang J, Liu H. Preparation and characterization of oligomeric char forming agent and its effect on the thermal degradation and flame retardant properties of LDPE with ammonium polyphosphate. *J Anal Appl Pyrolysis.* 2016;119:75-86.
 50. Wu W, Li M, Zhong Y, et al. Themoxidative stability and char formation mechanism for the introduction of CNTs and MoS₂ into halogen-free flame retarding TPEE. *RSC Adv.* 2016;6(4):3267-3275.

How to cite this article: Vahabi H, Shabaniyan M, Aryanasab F, et al. Three in one: β -cyclodextrin, nanohydroxyapatite, and a nitrogen-rich polymer integrated into a new flame retardant for poly (lactic acid). *Fire and Materials.* 2018;1-10. <https://doi.org/10.1002/fam.2513>